Transmittance thresholds of electrochromic glazing to achieve annual low-glare work environments

Jan Wienold*, Sneha Jain, Marilyne Andersen
Laboratory of Integrated Performance in Design (LIPID), Ecole Polytechnique Fédérale de Lausanne (EPFL), Lausanne, Switzerland
* *corresponding author: jan.wienold@epfl.ch*

Abstract

A recent study on the glare protection performance of electrochromic (EC) glazing showed that visible transmittance levels lower than 0.6% are necessary to achieve comfortable situations for sun positions, that were close to the central field of view. However, the question that arises is how often such situations occur throughout the year and how the glare protection performance of EC systems is for typical office situations for different climates and orientations. This study aims to quantify the annual performance for such configurations by applying improved simulation methods to conduct annual glare simulations and comparing them to the EN17037 classifications. The enhancement of the simulation method compared to existing methods was necessary to correctly consider the blurring effect in the lens of the eye – neglecting this would lead to an overestimation of glare.

We found that for mid and north European climates the extreme situations do not occur such often, so that the EC-glazing systems being able to switch to transmittance levels of 1% can mitigate glare throughout the year reasonably well for typical office situations and reaches typically the highest glare protection category according to EN17037 for a viewing direction, that is parallel to the facade. For more sunny climates such as Rome, slightly lower transmittance levels (around 0.5%) would be necessary to achieve a similar glare protection level.

The study also revealed that tables E.7 and E.8 of EN17037 with pre-calculated 95-percentile Daylight Glare Probability (DGP) values should be re-calculated.

Introduction

Electrochromic glazing (EC) is an emerging window technology that is applied to buildings to control solar radiation penetration for energy savings and thermal comfort (Ajaji & André, 2015; Piccolo, 2010). With its switchable transmittance technology, it offers control over the visual environment as well and therefore, can help in mitigating glare from daylight (Piccolo & Simone, 2009). There has been several studies based on simulations, physical measurements and occupant surveys to evaluate the capability of EC glazing in controlling discomfort glare (Clear et al., 2006; Jain et al., 2021; Lee & DiBartolomeo, 2002; Moeck et al., 1996). A recent user-assessment study (Jain et al., 2022) investigated the performance of such a façade system in terms of glare protection and found that it needs to be switched to transmittance levels below 0.6% to achieve comfortable situations if the sun is located in the central region of the field of view. Furthermore, the same study showed that 0.6% transmittance can achieve comfortable situations when the sun is in the peripheral field of view. The question that arises is: What should the annual glare protection performance of electrochromic glazing for typical workplace configurations be in different contexts? This study aims to answer that question and applies advanced annual glare simulations on different desk positions (distances from the window) and viewing directions, different orientations of the building and different geographic locations across three latitudes.

The European standard EN17037 that sets the requirements for providing adequate daylight into buildings (European Committee for Standardization CEN, 2019) also defines different levels of glare protection. Tables in its appendix provide precalculated 95-percentile Daylight Glare Probability (DGP) values for different orientations and climates, that should support planners to select appropriate transmittance levels to achieve the desired glare protection levels. However, the method applied to derive these values (the main author of this study was involved in deriving the tables in the standard) is ignoring the intraocular light scattering and therefore an overestimation of glare is expected.

In this study, with more accurate and sophisticated simulation methods we run simulations for the same geometry and climates in order to determine the needed transmittance levels of electrochromic glazing to meet the three comfort levels given by the EN17037 (low, medium and high). These outcomes support decision-making when it comes to building and workplace design using electrochromic glazing and help in setting boundaries if one wants to achieve low-glare environments with the use of such technology in different latitudes.

Method

Glare metric

For this study, the Daylight Glare Probability (DGP) metric is used to predict glare (Wienold & Christoffersen, 2006), as it is also used in EN17037 to define glare protection criteria. Several studies showed, that this metric is reliable to predict glare in typical workplace

situations (Jakubiec & Reinhart, 2012; Wienold et al., 2019) and specifically also for the usage of electrochromic glazing (Jain et al., 2022). For annual data on timestep-basis, we apply the method of EN17037 that uses the 95-percentile-value of the occurring DGP values during an assumed usage time between 08h-18h (note that in EN17037 this is the definition of "$DGP_{e<5\%}$").

Simulation method

To generate hourly DGP data, we applied a newly developed climate-based glare simulation method – the Adaptive Glare Coefficient method or AGC (Wienold & Andersen, 2022) – that uses hourly timesteps and is a speed-improved successor method of eDGPs (Wienold, 2009), showing similar behaviour and accuracy (Wasilewski et al., 2022).

Both methods (AGC and eDGPs) are based on RADIANCE (Ward, 1994) as the core rendering engine. The vertical illuminance E_v, a necessary input for both AGC and eDGPs, was calculated using Daysim. As most of the climate based daylight modelling tools (CBDM), the applied method relies on the Perez all weather sky model (Perez et al., 1993) for the sun and sky modelling.

Sun blurring

One crucial point for simulating glare when the sun is visible for the observer is the optical modelling of the "seen sun". While the simulated sun is a perfect disk with a view angle of 0.533°, the sun disk appears differently when in the field of view, due to the intraocular light scattering. Captured High Dynamic Images (HDR) images show a blurring effect, which is actually quite similar to what happens in the eye, where intraocular (forward) light scatter and internal reflections cause flare and an increase of the apparent size of the glare source. From an energy point of view, this blurring effect does not matter much since the energy flux remains nearly identical and, as a result, the core physical rule of energy conversion is kept. However, when it comes to the calculation of glare metrics, the blurring effect does matter due to the fact that most glare metrics including DGP use $L^2 \cdot \omega$ in their equation, while energy conservation follows $\sim L \cdot \omega$. The study at the basis of DGP used an HDR camera with a fish-eye lens that also caused the blurring of the sun – in other words, the "correct" calculation of DGP requires an image which blurs the sun. As consequence, a non-blurred sun in an HDR-image would automatically cause an overestimation of the glare.

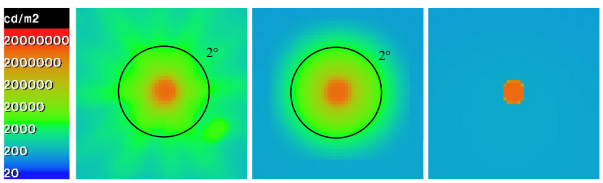

Figure 1: Visible sun behind EC glazing:
Left: Captured HDR image
Middle: Rendered image with sun blurring
Right: Rendered image without sun blurring

For that reason, we consider it necessary to integrate a blur effect in glare simulations if the sun disk may be visible in the field of view.

This was done in the AGC method, which has implemented a blurring feature based on Gaussian functions, which simulates a Lorentzian function with FWHM=11, introduced by (Ward et al., 2021).

In figure 1, we can visualize the luminance distributions around the sun disk for an HDR image, a simulation with and without blurring of the sundisk.

Figure 2 shows the energy flux as function of the integration angle around the sun direction for the captured HDR vs. the simulation, and illustrates that the Lorentzian approximation function follows closely the behaviour of the captured HDR image. It shows further, that within a 2° angle (=opening angle) around the sun direction (also illustrated in figure1), 98% of the sun + circumsolar (10°) energy is concentrated. Using *evalglare* to derive DGP from an image, it extracts peaks above a threshold of 50kcd/m^2 with its default setting, which translates for typical EC-situations to an angle of around 1° around sun direction for the extracted peak. Therefore, the Gaussian approach reproduces nearly an identical glare source compared to the captured image.

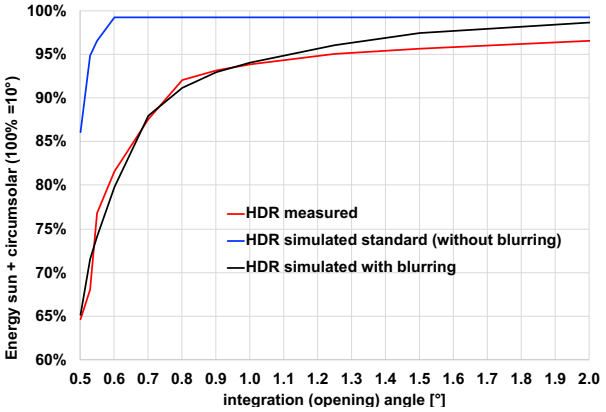

Figure 2: Energy of sun disk and circumsolar area for captured and simulated sun disk (with and without blurring) as function of the integration angle.

Model description

To re-build situations that can occur in open-plan offices, we used a wide-sized shoe-box model in the dimensions of 10m x 5m x 3m (width x depth x height), see figure 3. The simulated room is lit only from one side, the other walls are opaque (Reflection value: ρ=0.7, purely diffuse). The floor and ceiling were modelled with typical reflectance values, for Lambertian (purely diffuse) reflection: ρ_{floor}=0.2; $\rho_{ceiling}$=0.7.

The transparent façade was simplified using 2 horizontally divided panes of EC-glass without any frame in order to avoid any local shading effects. The lower pane (height 1.2m) was kept to τ_{vis}=0.2 for all timesteps. We used this height and constant transmittance value for the lower pane in order to achieve a reasonable amount of daylight while avoiding to increase the vertical

illuminance as much that it contributes significantly to the saturation term of the DGP. Although, we don't consider this "control strategy" of the lower pane as optimal for a building in terms of adequate solar control and daylight provision for deeper spaces, we found this a reasonable compromise for this study to balance daylight availability, saturation and contrast glare effects. Further investigations of optimal control strategies for EC facades are out of the scope of this study.

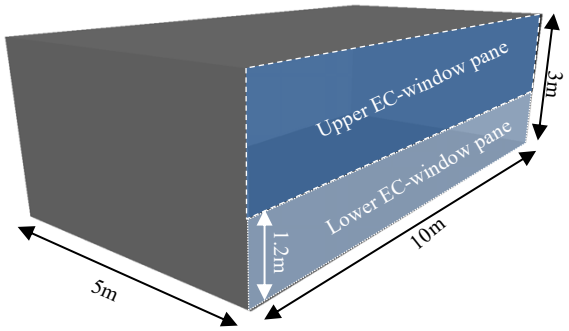

Figure 3: Visualization and dimensions of the room

Viewpoints and viewing directions

We simulated 6 viewpoints in total as two rows with 1, 2 and 3 m distance to the transparent façade and a distance of 1m each from the side wall (see illustration figure 4).

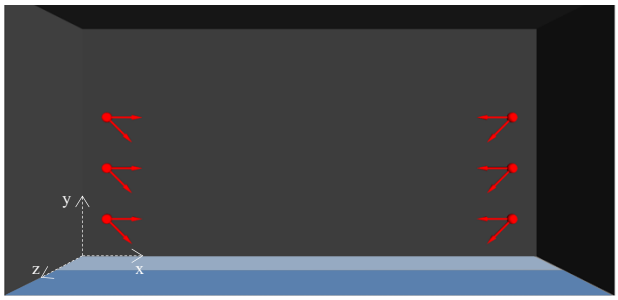

Figure 4: Top (perspective) view inside the shoebox: Visualization of the viewpoints and viewing directions.

We also simulated 2 different viewing directions: 1) parallel to the façade (labelled "P" following the naming in (Jain et al., 2022), with the sun present in the peripheral field of view) and 2) 45° from the façade (labelled "C" and mimicking a critical viewing direction in terms of increasing the glare risk with sun more frequently visible around the centre of the field of view).

We want to emphasize that the critical viewing direction "C" does not follow office layout recommendations and we also do not recommend such viewing directions. However, applying flexible office design options can lead to such situations and we think it is important to characterize the glare situations for such layouts as well.

Simulation variants

We conducted the simulations for three different locations in Europe to investigate the influence of latitude on glare classification:

Stockholm (59.35N, 18.07E), Frankfurt (50.03N, 8.52E) and Rome (41.90N, 12.48E). We used the *.wea* weather files provided by Climate.OneBuilding.Org, ids: Stockholm.024850, Frankfurt.AP.106370, Rome.Central.162380).

Our simulations include four different orientations of EC façade: South (S), South-West (SW), West (W) and North-West (NW). These orientations are selected to consider critical sun positions in terms of glare at the chosen locations.

For the upper window, we simulated 15 different tint levels, that were each kept constant throughout the entire year of simulation. This setting of the glazing transmittance does not correspond to a real control strategy of the EC-facade of course. In this study, we focused instead on determining the tint level needed to provide sufficient glare protection – for this goal a fixed transmittance level setting throughout the year is appropriate. We simulated following transmittance levels of τ_{vis}:

0.1%, 0.25%, 0.5%, 0.75%, 1%, 1.25%, 1.5%, 2%, 3%, 4%, 5%, 6%, 10%, 15% and 20%.

In total, 360 annual simulation runs were conducted (3 locations x 4 orientations x 2 viewing directions x 15 transmittance levels, the 6 viewpoints were calculated within one simulation run).

The 95-percentile DGP values are determined for each viewpoint and simulation variant separately. Out of the two viewpoints located at the same distance from the façade, the higher percentile value is reported in this study (reporting therefore the more critical position out of the two with same distance). The applied method, models and locations corresponds to the procedure that was applied deriving the tables E.7 and E.8 of the appendix of EN17037, the main author of this paper was also involved in the development of the standard.

Results

Influence of orientation and viewing direction

The figures 5-7 visualize the annual 95-percentile values of DGP as function of the glazing transmittance for the three locations, four orientations and two viewing directions (all curves are for a viewing position in 1m distance of the façade). The three glare protection categories of EN17037 are highlighted with a coloured background (minimum=orange (DGP=0.45), medium=yellow (DGP=0.40) and high=green (DGP=0.35)). For the Stockholm and Frankfurt locations, the different orientations have only little impact on the annual glare occurrence for the less critical parallel viewing direction. For the diagonal viewing direction, however, a tendency towards higher values for the West and South-West orientations can be observed for all locations. For all locations and both viewing directions, we can also see that the curves of South and West orientation are either higher or similar than the other two orientations: this means those two orientations are the most important ones to consider for glare evaluations without missing important glare occurrences. As

expected, the curves associated to critical viewing direction are significantly higher than the curves for the parallel viewing direction.

The colour scale of the background of figure 5-11 indicates the glare protection class according to EN17037:

high glare protection | medium glare protection | minimum glare protection | no glare protection

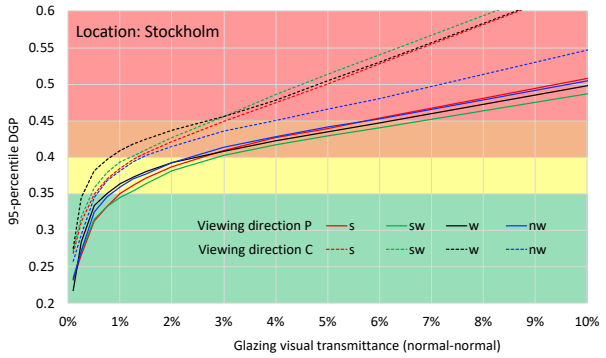

Figure 5: 95-percentile DGP as function of the glazing transmittance for Stockholm and for different orientations (s=South, sw=South-West, w=West, nw=North-West) and viewing directions (P=parallel view, C=critical view (45° towards façade)).

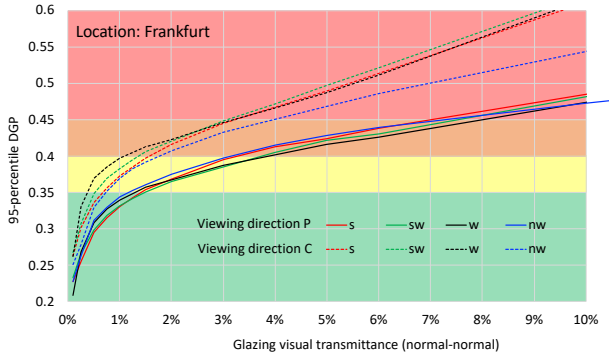

Figure 6: 95-percentile DGP as function of the glazing transmittance for Frankfurt and for different orientations (s=South, sw=South-West, w=West, nw=North-West) and viewing directions (P=parallel view, C=critical view (45° towards façade))

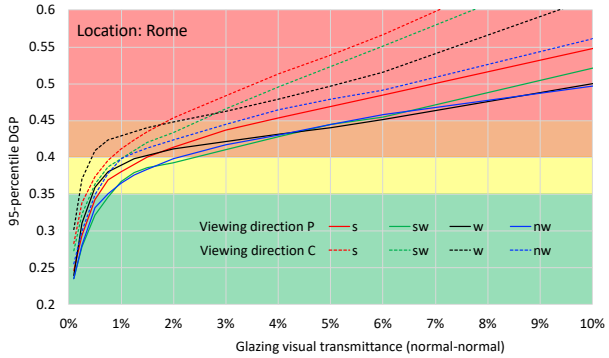

Figure 7: 95-percentile DGP as function of the glazing transmittance for Rome and for different orientations (s=South, sw=South-West, w=West, nw=North-West) and viewing directions (P=parallel view, C=critical view (45° towards façade)).

Influence of observer distance

Figures 8-11 show the impact of observer distance to the façade on the annual glare occurrence for South and West orientations in Frankfurt and Rome. For this evaluation we needed to reduce the cases to be compared. We kept the two extreme climates (omitting Stockholm) and two main orientations (omitting South-West and North-West). From 0 up until around 3% transmittance, the curves are mainly driven by the geometrical configuration influencing how often the sun disk is potentially visible by the observer. As a result, the curves for 1m and 2m are lying very close to each other for all cases. For a viewing position 3m from the window, we can observe lower values, which is caused by a reduced view to the sky due to geometry.

For transmittance levels higher than 3%, the saturation term in the DGP equation gets more influence and therefore the annual glare occurrence depends significantly on the induced vertical illuminance: deeper room locations experience less glare and the curves drift away from each other for high transmittance levels.

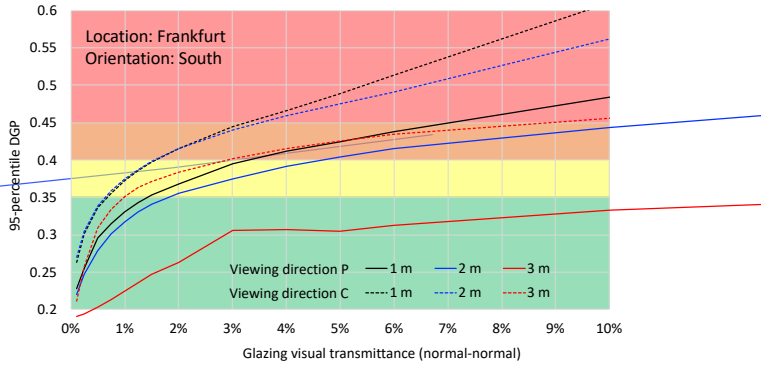

Figure 8: 95-percentile DGP as function of the glazing transmittance for Frankfurt (South orientation) and different façade distances

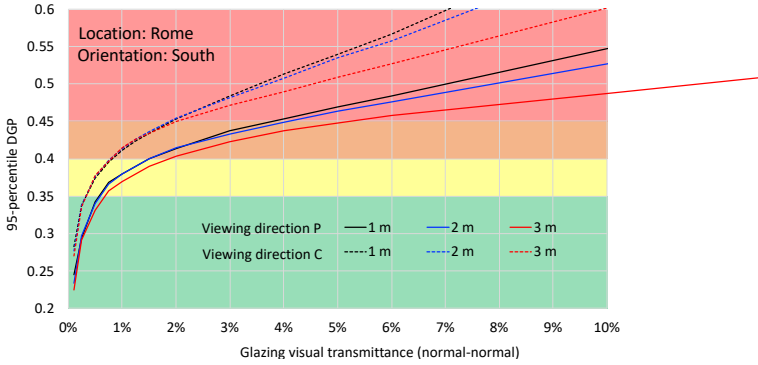

Figure 9: 95-percentile DGP as function of the glazing transmittance for Rome (South orientation) and different façade distances

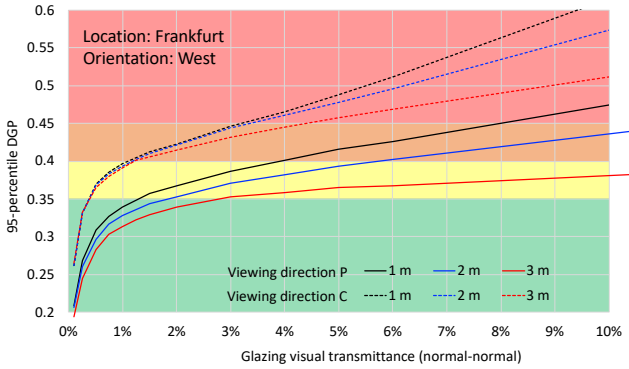

Figure 10: 95-percentile DGP as function of the glazing transmittance for Frankfurt (West orientation) and different façade distances

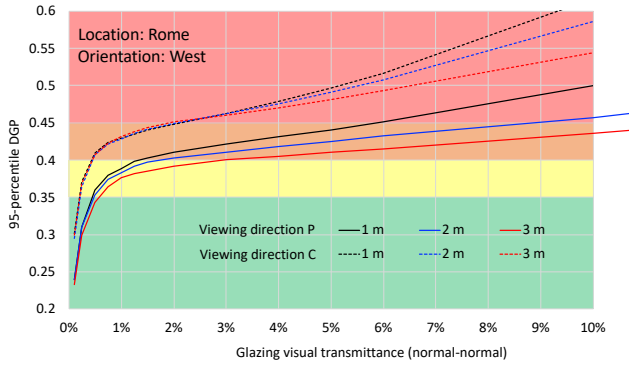

Figure 11: 95-percentile DGP as function of the glazing transmittance for Rome (West orientation) and different façade distances

Influence of latitude/climate

As can be seen in Figure 12 and 13, the annual glare-behaviour of the three climates differ significantly – with Rome showing highest glare risks, followed by Stockholm and Frankfurt having the lowest glare risk amongst the three climates.

This ranking could be expected considering the sunshine hours of the three locations (Rome: 3740h, Stockholm 2187h and Frankfurt 1748h, calculated from the weather files accounting for sunshine hours when the direct solar irradiance exceeds 120 W/m^2 (WMO 2018)).

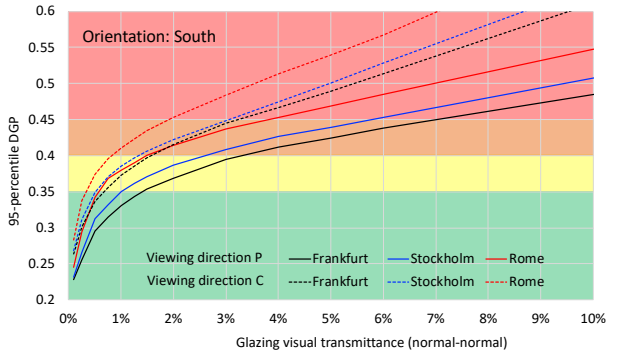

Figure 12: 95-percentile DGP as function of the glazing transmittance for different climates and two viewing directions. All values for South orientations and 1m distance to the façade.

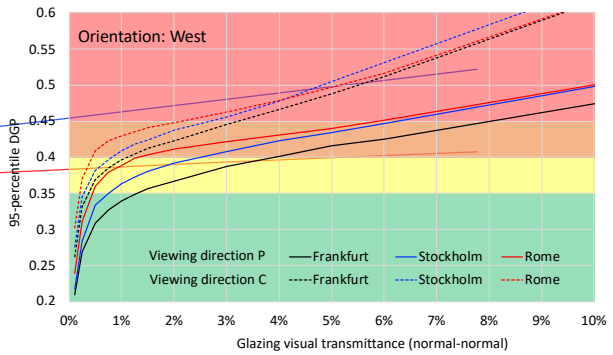

Figure 13: 95-percentile DGP as function of the glazing transmittance for different climates and two viewing directions. All values for West orientations and 1m distance to the façade.

Discussion

The results suggest that for the parallel viewing direction (that is usually recommended) a transmittance level of 1% is sufficient to achieve the highest glare protection classification according to EN17037 for Stockholm and Frankfurt. For Rome a transmittance level of 0.5% would be need to achieve the highest glare protection classification.

For the critical, diagonal viewing direction, the behaviour is similar except that one class lower glare protection is reached for the same transmittance level (1% for Frankfurt and Stockholm, 0.5% for Rome, medium glare protection is then reached, EN17037).

To reach the minimum glare protection category according to EN17037 (DGP 95percentile < 0.45), a transmittance level of 4% is sufficient for the parallel viewing direction and 2% for the critical viewing direction – independent on climate and orientation.

These results emphasize how important it is to investigate glare behaviour on annual basis and not just for some selected, critical cases. While the simulation model is able to reproduce the findings from Jain et. al 2022 quite well for critical sun positions, the annual results reveal that it strongly depends on the climate how often these critical situations occur and if a certain transmittance level of the glazing system is sufficient to fulfil the criteria given by EN17037.

Comparing the detailed results with tables E.7 and E.8 (corrigendum from 2021), one can see deviations in the calculated 95-percentiles of the DGP values (tables 1,2).

These deviations are caused by three influence factors:

1. The calculations for the EN17037 were conducted without any sun-blurring, which results in higher DGP values for the same boundary conditions.
2. For the calculations for the EN17037, the entire window pane was dimmed, whereas for the simulations in this study, parts of the window were in maximum bleached state in order to provide sufficient daylight. A complete dimming

causes a very low E_v for low switching levels, which impacts the contrast term of the DGP equation by increasing the DGP value compared to a more reasonable E_v.

3. The simulations for the EN17037 used the default mode of *evalglare* (version 2.04) applying a so called "low-light-correction" (Wienold 2012), which decreases the DGP value for E_v values lower than 500lux. That causes a significant underprediction of the DGP value for very low switching levels (1% or lower).

These three influence factors lead to important deviations between the values calculated for this study (which we see as state-of-the-art results) and the tables E.7 and E.8 of the EN17037. This finding suggests that an update of the tables in the standard will be necessary for the next revision.

Table 1: Comparison between EN17037 and this study of calculated 95percentile DGP values between 08h-18h for Frankfurt, parallel viewing direction and selected transmittance values. The used window size in this study corresponds to the large window size in EN17037.

LOCATION: FRANKFURT (SUNSHINEZONE L ACCORDING TO EN17037) VIEWING DIRECTION: PARALLEL TO FACADE									
		Orientation South				Orientation West			
Distance to facade		τ_{vis} 1%	τ_{vis} 2%	τ_{vis} 3%	τ_{vis} 5%	τ_{vis} 1%	τ_{vis} 2%	τ_{vis} 3%	τ_{vis} 5%
1m	EN17037	<0.2	0.42	0.46	0.51	<0.2	0.43	0.47	0.51
	This study	0.33	0.37	0.39	0.42	0.34	0.37	0.39	0.42
2m	EN17037	<0.2	0.22	0.40	0.47	<0.2	0.36	0.45	0.49
	This study	0.32	0.36	0.37	0.40	0.33	0.35	0.37	0.39
3m	EN17037	<0.2	<0.2	<0.2	0.31	<0.2	<0.2	0.25	0.44
	This study	0.22	0.26	0.31	0.30	0.31	0.34	0.35	0.36

Table 2: Comparison between EN17037 and this study of calculated 95percentile DGP values between 08h-18h for Rome, parallel viewing direction and selected transmittance values. The used window size in this study corresponds to the large window size in EN17037.

LOCATION: ROME (SUNSHINEZONE H ACCORDING TO EN17037) VIEWING DIRECTION: PARALLEL TO FACADE									
		Orientation South				Orientation West			
Distance to facade		τ_{vis} 1%	τ_{vis} 2%	τ_{vis} 3%	τ_{vis} 5%	τ_{vis} 1%	τ_{vis} 2%	τ_{vis} 3%	τ_{vis} 5%
1m	EN17037	0.24	0.47	0.50	0.50	0.23	0.47	0.50	0.53
	This study	0.38	0.41	0.44	0.47	0.39	0.41	0.42	0.44
2m	EN17037	<0.2	0.45	0.49	0.51	<0.2	0.43	0.49	0.52
	This study	0.38	0.41	0.46	0.46	0.38	0.40	0.41	0.42
3m	EN17037	<0.2	0.32	0.46	0.50	<0.2	0.33	0.47	0.50
	This study	0.37	0.40	0.45	0.45	0.38	0.39	0.40	0.41

Another interesting result is that the glare occurrence for the three climates are so different. To further explain this result, one has to remember the contrast term in the DGP equation, which is proportional to $L^2 \cdot \omega/(E_v^{1.87} \cdot P^2)$ with L: luminance, w: solid angle, E_v: vertical illuminance at eye level; P: Position index. While the solid angle for the glare source (=visible sun disk) is the same for all climates and independent of time of the day/year, the sun position and therefore the Position index is different between the different locations. For the 95-percentile DGP value, what matters the most is therefore how often the sun-disk is visible throughout the year (and between 8h-18h), and how often sun-luminance is high while the position index is low. We defined the sun luminance as "high", using the 25-percentile of the sun disk luminance in the EC-experiment (Jain et. al 2022) to $6.25 \cdot 10^8$ cd/m^2 (which is around 25% of the maximum possible, extraterrestrial luminance of the sun of $2.43 \cdot 10^9$ cd/m^2 as seen from earth). We define a "low position index" for values 1-4, resulting in a maximum "reduction" of the contrast term by around 1.5 orders of magnitude (P=4 means to divide by 16 in the contrast term $\sim log\ \frac{L^2\omega}{E_v^{1.87}P^2}$)

With these definitions, we calculated the number of hours per year when the sun is visible during 08h-18h and strong enough (exceeding luminance threshold and below Position index threshold) to cause glare for the West orientation and the critical viewing direction. We found for Stockholm 158h, for Rome 191h and for Frankfurt 126h per year critical for glare.

In the following figures 14-16, the representations of position index and the temporal occurrence confirm that for Frankfurt, significantly less hours of critical sun conditions occur than for the other two climates.

Although the sunshine hours for the climates show a similar trend, we assume that considering only critical sun conditions (high intensity and low position index) for a climate-classification is the more accurate approach since it uses only the relevant data. This should be investigated further.

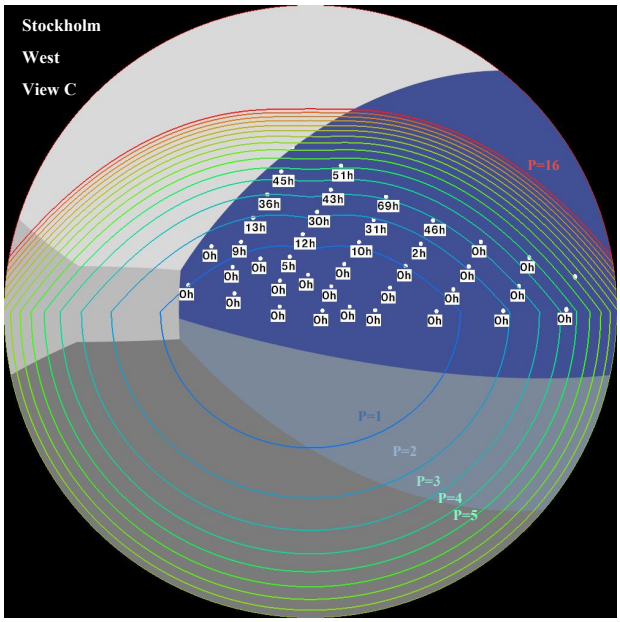

Figure 14: Visualization of visible sun position (little white dots) for the critical viewing direction C, number of critical hours between 8-18 where the sun luminance is > $6.25 \cdot 10^8$ cd/m^2 and the position index as isolines for Stockholm and West-Orientation.

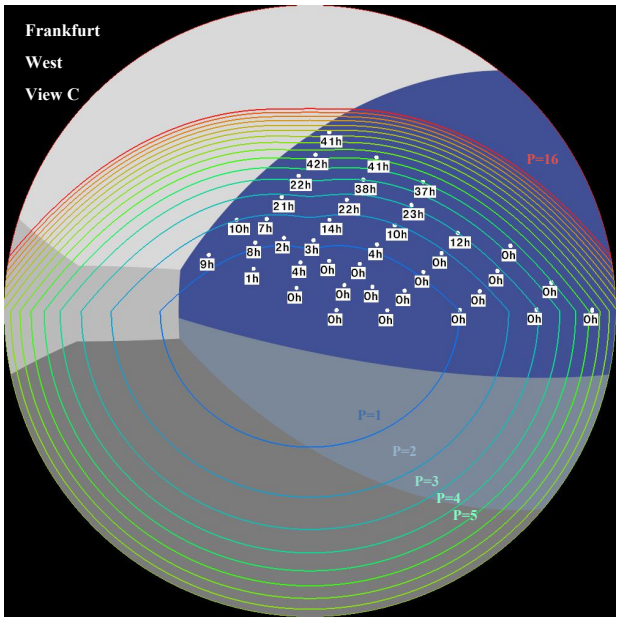

Figure 15: Visualization of visible sun position (little white dots) for the critical viewing direction C, number of critical hours between 8-18 where the sun luminance is > 6.25·10^8 cd/m^2 and the position index as isolines for Frankfurt and West-Orientation.

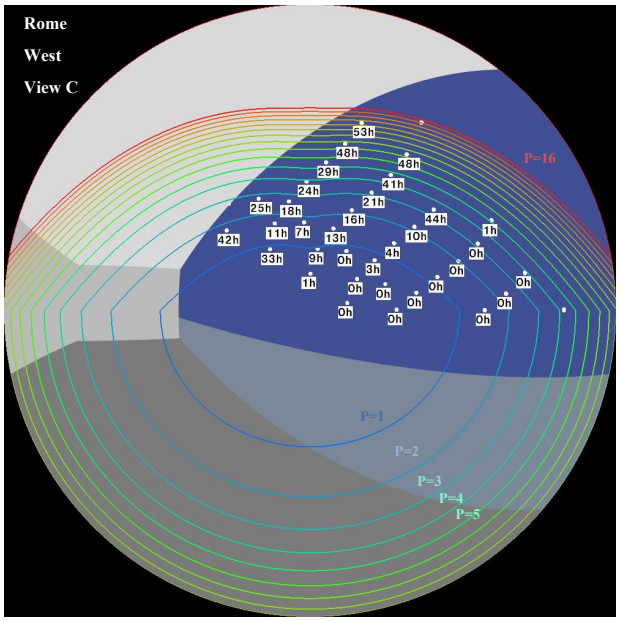

Figure 16: Visualization of visible sun position (little white dots) for the critical viewing direction C, number of critical hours between 8-18 where the sun luminance is > 6.25·10^8 cd/m^2 and the position index as isolines for Rome and West-Orientation.

Limitations

Current findings (Wienold & Jain 2021) suggest, that existing glare metrics like DGP reproduce discomfort perception of people reasonably well for blue tinting EC glazing, but also suggest that neutrally tinted glazing have lesser glare impact than the blue tinting ones. For that reason, the findings presented in this study are valid for blue tinting glazing and might differ if a prediction model considering colour effects on glare is available.

All findings are impacted by the peak extraction algorithm and threshold, applied by *evalglare*. Applying a lower threshold or defining a fixed cone around the sun direction for the glare source could lead to a decrease of the DGP value due to the $L^2 \cdot \omega$ proportionality of the contrast term of most glare equations incl. DGP. The existing default threshold for peak extraction of 50kcd/m^2 was a reasonable setting for the development data of the DGP, but no study exists yet showing that this value is also the "right" setting for situations when the sun-disk is visible. The application of a gradient-driven peak extraction algorithm might be a better solution to extract a peak than using a fixed threshold, that changes size when having different tinting levels. Applying different algorithms to data with a visible sun disk will probably reduce the DGP values and therefore better reproduce the thresholds found for such cases in user studies (Jain et al. 2022).

Conclusion

This study has shown that existing EC-glazing systems able to switch to transmittance levels of 1% can mitigate glare throughout the year reasonably well for typical office situations (viewing direction parallel to the window) in mid and northern European climates.

For sunny climates as Rome (and typical office situations), a 1% transmittance level reaches the medium glare protection category according to EN17037 for all orientations.

For a critical viewing direction (which is not a recommended desk position), the usage of 1% transmittance is typically enough to reach the medium glare protection level of the EN17037 in mid and northern European climates. For the sunny climate the usage of 1% transmittance level leads to fulfil the minimum glare protection level.

The study also revealed that tables E.7 and E.8 of EN17037 with pre-calculated 95-percentile DGP values should be updated using state-of-the-art methods. As shown in tables 1 and 2, we found higher glare thresholds for parallel viewing direction compared to EN17037 for VLT=1%. Whereas we found lower glare thresholds for VLT>=2% in this study compared to EN17037.

The deviations in values are significant and are caused by the method applied for deriving the EN17037 values and result from a combination of the following factors: a) non-sun blurring b) full tinting of all glass panes causing low adaptation levels c) using default low-light correction function in *evalglare*.

Another important conclusion is the importance of conducting annual simulation to investigate the performance of glare protection systems. Considering only critical conditions might lead to different conclusions and potentially to an "oversizing" of shading systems. However, considering the large variability

between human occupants in terms of glare perception, the application of user-adjustable control algorithms for a dynamic shading system to adjust to individual needs will definitely increase the acceptability – independently of the technology (e.g. EC, fabric or Venetian blinds) used for glare protection.

Acknowledgement

This study was funded by Swiss National Foundation project (SNF) grant for the project "Visual comfort without borders: interactions on discomfort glare" number 200020_182151.

References

Ajaji, Y., & André, P. (2015). Thermal Comfort and Visual Comfort in an Office Building Equipped with Smart Electrochromic Glazing: An Experimental Study. *Energy Procedia*, *78*, 2464–2469. https://doi.org/10.1016/j.egypro.2015.11.230

Clear, R. D., Inkarojrit, V., & Lee, E. S. (2006). Subject responses to electrochromic windows. *Energy and Buildings*, *38*(7), 758–779. https://doi.org/10.1016/j.enbuild.2006.03.011

European Committee for Standardization CEN. (2019). *EN17037:2019 Daylight in buildings*.

Jain, S., Karmann, C., & Wienold, J. (2021). Subjective assessment of visual comfort in a daylit workplace with an electrochromic glazed façade. *Journal of Physics: Conference Series*, *2042*(1), 012179. https://doi.org/10.1088/1742-6596/2042/1/012179

Jain, S., Karmann, C., & Wienold, J. (2022). Behind electrochromic glazing: Assessing user's perception of glare from the sun in a controlled environment. *Energy and Buildings*, *256*, 111738. https://doi.org/10.1016/j.enbuild.2021.111738

Jakubiec, J., & Reinhart, C. (2012). The 'adaptive zone'—A concept for assessing discomfort glare throughout daylit spaces. *Lighting Research and Technology*, *44*(2), 149–170. https://doi.org/10.1177/1477153511420097

Lee, E. S., & DiBartolomeo, D. L. (2002). Application issues for large-area electrochromic windows in commercial buildings. *Solar Energy Materials and Solar Cells*, *71*(4), 465–491. https://doi.org/10.1016/S0927-0248(01)00101-5

Moeck, M., Lee, E. S., Rubin, M. D., Sullivan, R., & Selkowitz, S. E. (1996). *Visual quality assessment of electrochromic and conventional glazings* (LBNL-39471; CONF-9609325-4). Lawrence Berkeley National Lab., CA (United States). https://www.osti.gov/biblio/474886

Perez, R., Seals, R., & Michalsky, J. (1993). All-weather model for sky luminance distribution—Preliminary configuration and validation. *Solar Energy*, *50*(3), 235–245. https://doi.org/10.1016/0038-092X(93)90017-I

Piccolo, A. (2010). Thermal performance of an electrochromic smart window tested in an environmental test cell. *Energy and Buildings*, *42*(9), 1409–1417. https://doi.org/10.1016/j.enbuild.2010.03.010

Piccolo, A., & Simone, F. (2009). Effect of switchable glazing on discomfort glare from windows. *Building and Environment*, *44*(6), 1171–1180. https://doi.org/10.1016/j.buildenv.2008.08.013

Ward, G. J. (1994). The RADIANCE lighting simulation and rendering system. *Proceedings of the 21st Annual Conference on Computer Graphics and Interactive Techniques - SIGGRAPH '94*, 459–472. https://doi.org/10.1145/192161.192286

Ward, G. J., Wang, T., Geisler-Moroder, D., Lee, E. S., Grobe, L. O., Wienold, J., & Jonsson, J. C. (2021). Modeling specular transmission of complex fenestration systems with data-driven BSDFs. *Building and Environment*, *196*, 107774. https://doi.org/10.1016/j.buildenv.2021.107774

Wasilewski, S., Wienold, J. & Andersen, M. (2022) Critical Comparison of Annual Glare Simulation Methods. *Submitted to the IBPSA-Nordic Conference 2022*, Copenhagen, DK

Wienold, J. (2009). Dynamic daylight glare evaluation. *Proceedings of Building Simulation*, 944–951.

Wienold, J., & Christoffersen, J. (2006). Evaluation methods and development of a new glare prediction model for daylight environments with the use of CCD cameras. *Energy and Buildings*, *38*(7), 743–757. https://doi.org/10.1016/j.enbuild.2006.03.017

Wienold, J. (2012), New features of evalglare. *11th International Radiance Workshop*. Copenhagen, Denmark. September 12-14, 2012.

Wienold, J., Iwata, T., Sarey Khanie, M., Erell, E., Kaftan, E., Rodriguez, R., Yamin Garreton, J., Tzempelikos, T., Konstantzos, I., Christoffersen, J., Kuhn, T., Pierson, C., & Andersen, M. (2019). Cross-validation and robustness of daylight glare metrics. *Lighting Research & Technology*, *51*(7), 983–1013. https://doi.org/10.1177/1477153519826003

Wienold, J. & Jain, S. 2021, Glare behind (blue) electrochromic glazing: Do we know how it is perceived? Do we know how we simulate? And do we know what we measure? *19th International Radiance Workshop*. Bilbao, Spain. August 19-20, 2021.

Wienold, J. & Andersen, M. (2022), Adaptive glare coefficient method for climate-based daylight glare analyses. To be submitted before summer 2022.

World Meteorological Organization WMO (2018), Guide to Instruments and Methods of Observation (WMO-No. 8), ISBN: 978-92-63-10008-5.